Nature of Deep Earthquakes in the Pacific Plate from Unsupervised Machine Learning

Gilbert Mao[1] and Gilbert Mao[1]

[1]William Mason High School

November 22, 2022

Abstract

Deep earthquakes, 300 to 700 km deep, have been observed for decades and shown to originate from major mineral transformations occurring at these depths, including phase transitions of olivine and pyroxenes. Yet, we still do not fully grasp their mechanism. Although transformational faulting in the rim of the metastable olivine wedge (MOW) is hypothesized as a triggering mechanism of deep-focus earthquakes, there is no direct seismic evidence of such rim. Variations of b-value – slope of the Gutenberg-Richter distribution – have been used to decipher triggering and rupture mechanisms of earthquakes. However, regarding deep-focus earthquakes the detection limit prevents full understanding of rupture nucleation at all sizes. With one of the most complete catalogs, the Japan Meteorological Agency (JMA) catalog, we estimate the b values of deep-focus earthquakes ($>$ 300 km) of four clusters in the NW Pacific Plate based on unsupervised machine learning. The applied K-means algorithm divides the events into four clusters. For the first time, we observe kinks in the b values with abrupt reductions from 1.5–1.8 down to 0.7–1.0 at a threshold Mw of 3.7–3.8 for the Honshu and Izu clusters, while normal constant b values (0.9–1.0) are observed for the Bonin and Kuril clusters. The four clusters found by the algorithm actually correspond to events within four different segments of the sinking Pacific lithosphere, characterized by significant differences in hydration state prior to subduction. High b values (1.5–1.8) at low magnitudes (Mw $<$ 3.7–3.8) correlate with highly hydrated slab portions. The hydrous defects would enhance the nucleation of small earthquakes via transformational faulting within the rim. Such mechanism operates for small events with a rupture length of less than 1 km, which would correspond to the thickness of the MOW rim. Combining with the b-value analysis from the latest CMT catalog, the kink at Mw 6.7 suggests that the thermal runaway mechanism operates for larger earthquakes rupturing through and possibly propagating outside the MOW, with increased heterogeneity in the new rupture domain. The changes of controlling mechanism and rupture domain heterogeneity due to the slab hydrous state and thermal state can explain the spatially varying b values.

S45F-0378

Nature of Deep Earthquakes in the Pacific Plate from Unsupervised Machine Learning

Gilbert Mao[1,2], Thomas P. Ferrand[3,4], Jiaqi Li[1,5], Brian Zhu[1,6], Ziyi Xi[1] and Min Chen[1,7]

(1) Department of Computational Mathematics, Science and Engineering, Michigan State University, East Lansing, MI 48824, USA; (2) William Mason High School, Mason, OH, 45040, USA; (3) Institute of Geological Sciences, Freie Universität Berlin, 12249 Berlin, Germany; (4) Institut des Sciences de la Terre d'Orléans, UMR-7327, Université d'Orléans – CNRS, Orléans, France; (5) Department of Earth, Planetary, and Space Sciences, University of California, Los Angeles, CA 90095, USA; (6) Department of Statistics and Data Science, Yale University, New Haven, CT 06520, USA; (7) Department of Earth and Environmental Sciences, Michigan State University, East Lansing, MI 48824, USA

INTRODUCTION

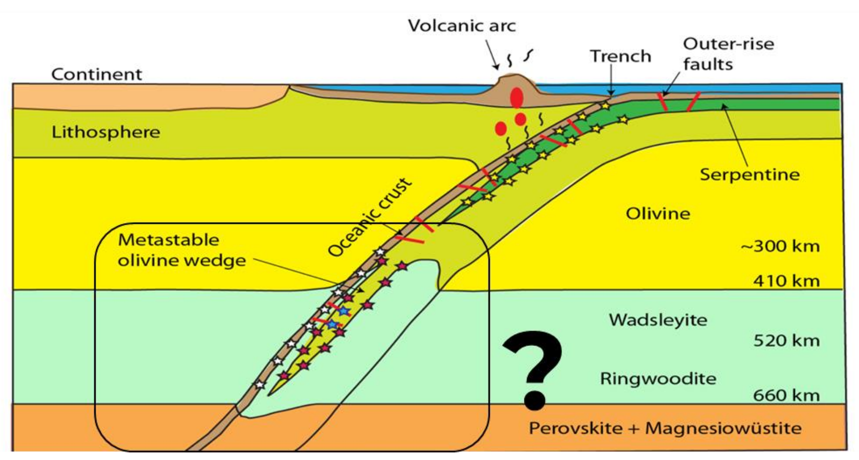

1. thermal shear instability
2. dehydration embrittlement
3. transformational faulting

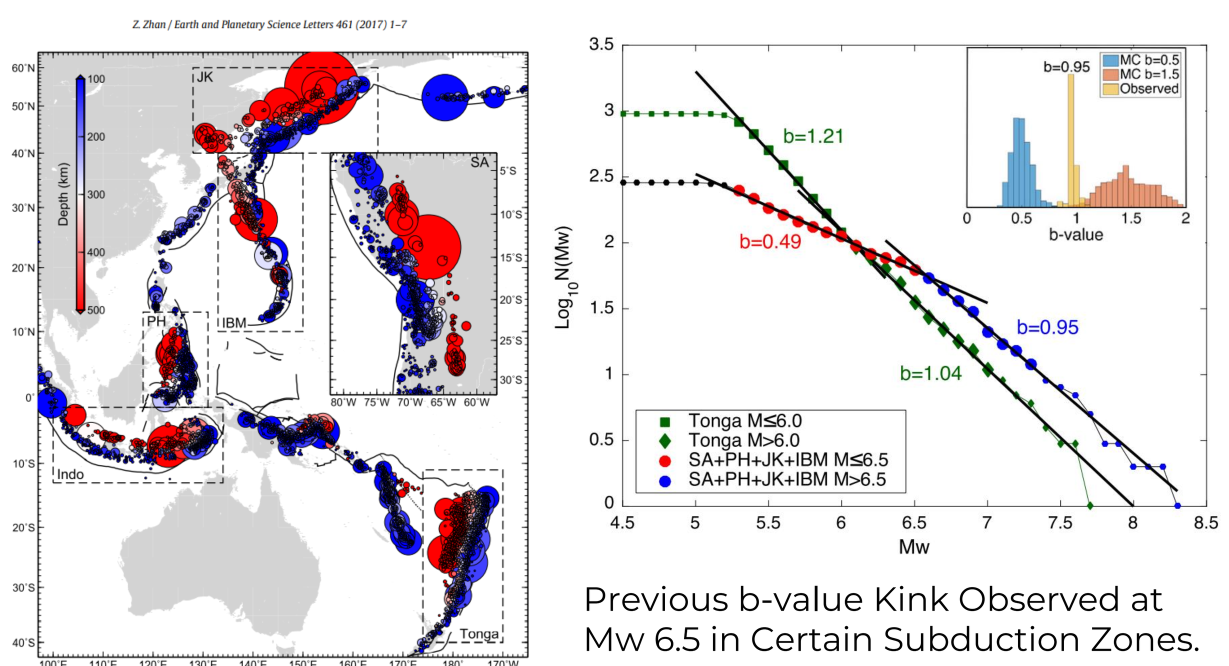

Previous b-value Kink Observed at Mw 6.5 in Certain Subduction Zones.

Dual Mechanism Hypothesis Based on b-value Analysis of CMT Catalog

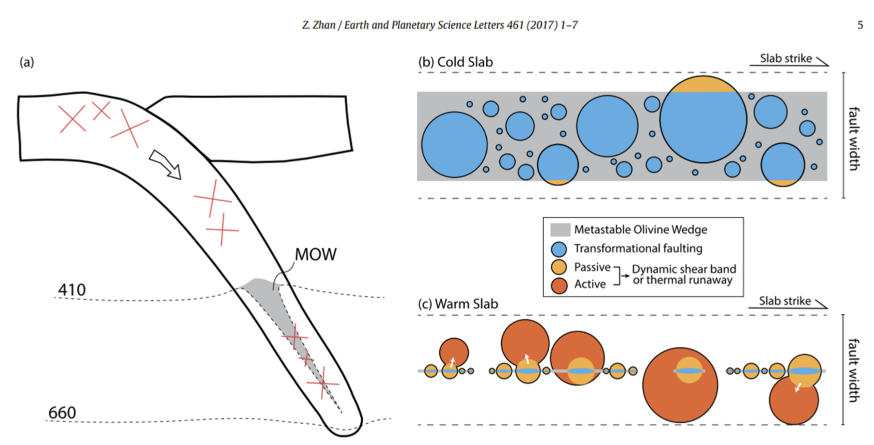

Data & Analysis

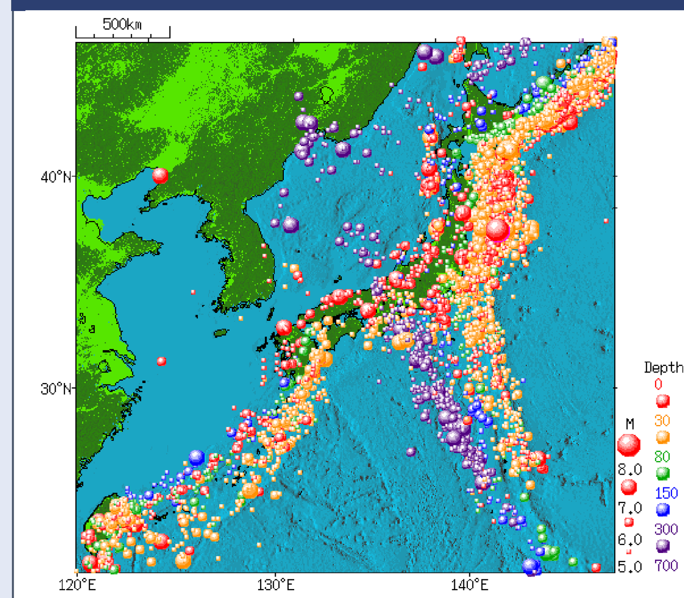

- More complete earthquake catalog for Japan and its surrounding regions
- JMA magnitude (Mj) has been converted to Mw (Uchide & Imanishi, 2018)

$$M_w = aM_j^2 + bM_j + c.$$

$a = 0.053 \pm 0.003$, $b = 0.33 \pm 0.02$, and $c = 1.68 \pm 0.03$

- JMA Earthquake Magnitude of Completeness (Mc ~ 3.3) much lower than CMT catalog (Mc ~ 5)
- Over two million earthquakes

Clustering Analysis with Unsupervised Machine Learning:

***K*-means Clustering**

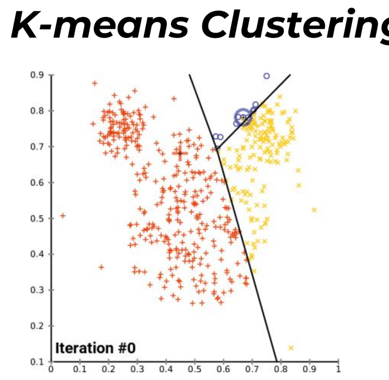

1. Initialize k random centroids
2. Create clusters
3. Recalculate the centroids
4. Repeat until convergence.

Silhouette Score

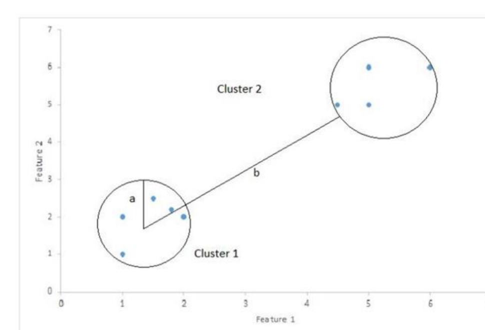

Silhouette Score = (b-a)/max(a,b)
a= average intra-cluster distance
b= average inter-cluster distance

Spectral Clustering

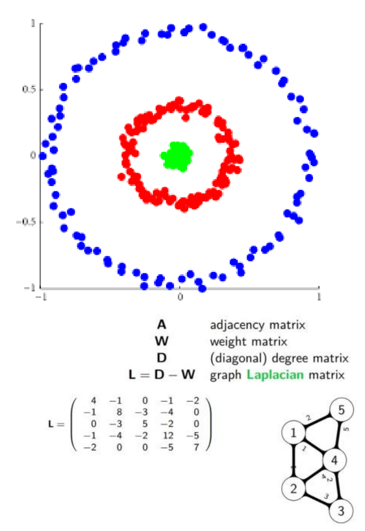

b-value analysis and its error analysis:

$$b_0 = \frac{1}{\ln(10)*(\mu - M_c)} \qquad \sigma_{b_0} = 2.3{b_0}^2\sqrt{\frac{\sum_{i=1}^{N}(M_i-\mu)^2}{N(N-1)}}$$

$$b_1 = \frac{1}{\ln(10)*(\mu-(M_c-\Delta M/2))} \qquad \sigma_{b_1} = 2.3{b_1}^2\sqrt{\frac{\sum_{i=1}^{N}(M_i-\mu)^2}{N(N-1)}}$$

$$b_2 = \frac{1}{\ln(10)*\Delta M} * \ln\left(1+\frac{\Delta M}{\mu-M_c}\right) \qquad \sigma_{b_2} = \frac{\frac{\Delta M}{\mu-M_c}}{\ln(10)*\Delta M*\sqrt{N*(1+\frac{\Delta M}{\mu-M_c})}}$$

Gaussian Mixture Models Clustering

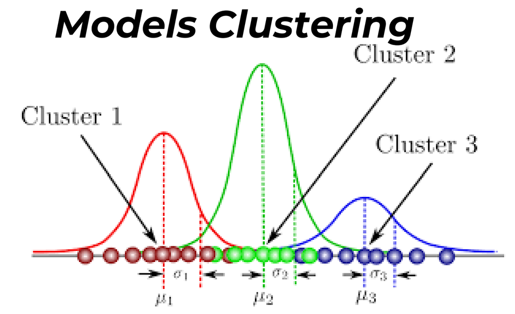

Mechanisms for the *b*-value Kinks

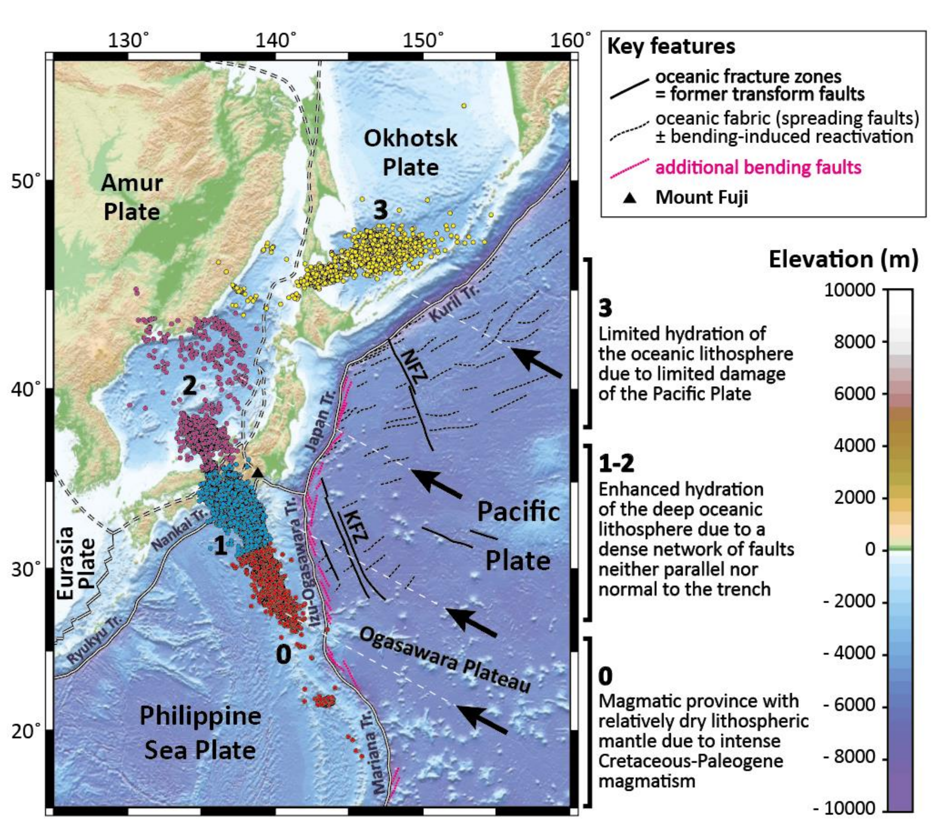

Pre-Subducting Plate Hydration Affects the Water Abundance in the MOW Halo.

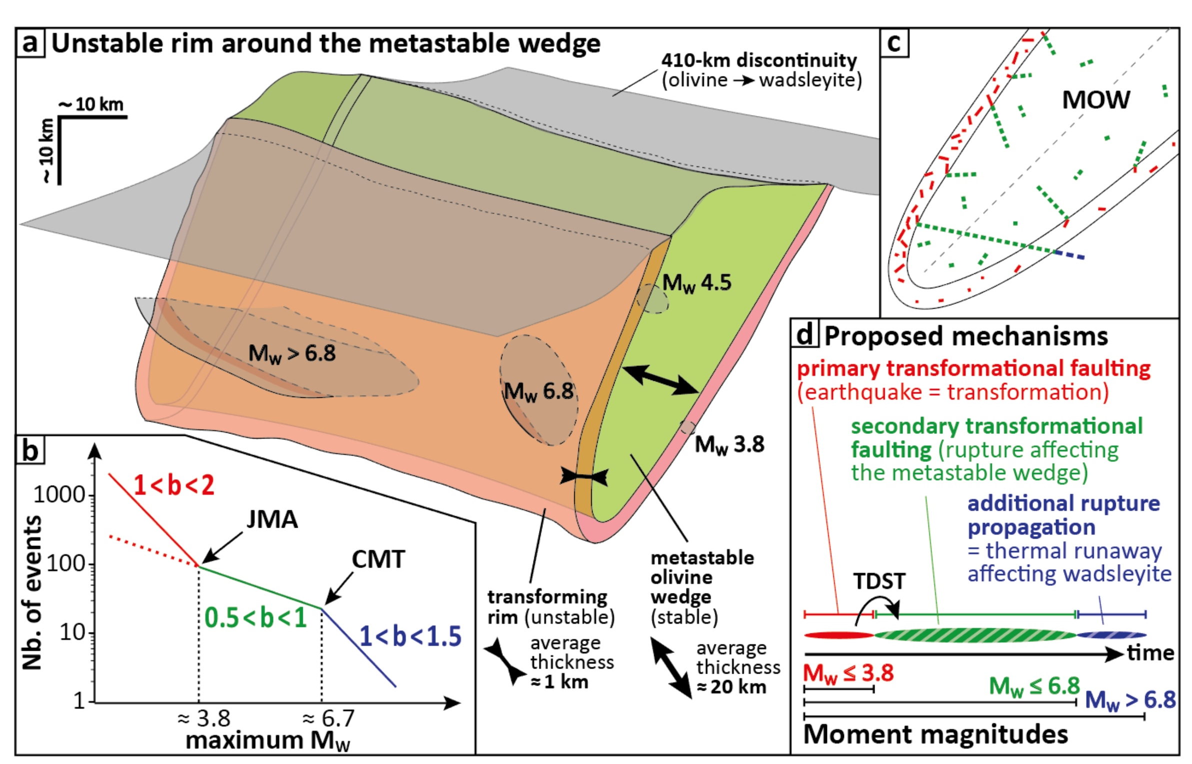

Deep-Focus Earthquakes Triggered in the Unstable Transforming Rim and can Propagate Into and then Outside the MOW. Water Acts as a Catalyst of Small Earthquakes in a Highly Reactive Halo of MOW.

References

1. Zhan, Z. Gutenberg–Richter law for deep earthquakes revisited: A dual-mechanism hypothesis. *Earth Planet. Sci. Lett.* **461**, 1–7 (2017).
2. Ishii, T. & Ohtani, E. Dry metastable olivine and slab deformation in a wet subducting slab. *Nature Geoscience* **14**, 526–530 (2021).
3. Warner., M. & Sandri, L., A review and new insights on the estimation of the b-value and its uncertainty. *Annals of Geophysics* **46**(6) (2003).
4. Ferrand, T. P. *et al.* Dehydration-driven stress transfer triggers intermediate-depth earthquakes. *Nature Communication* **8**, 1–11 (2017).

Results & Conclusion

K-means Clustering Analysis and *b*-value Analysis:

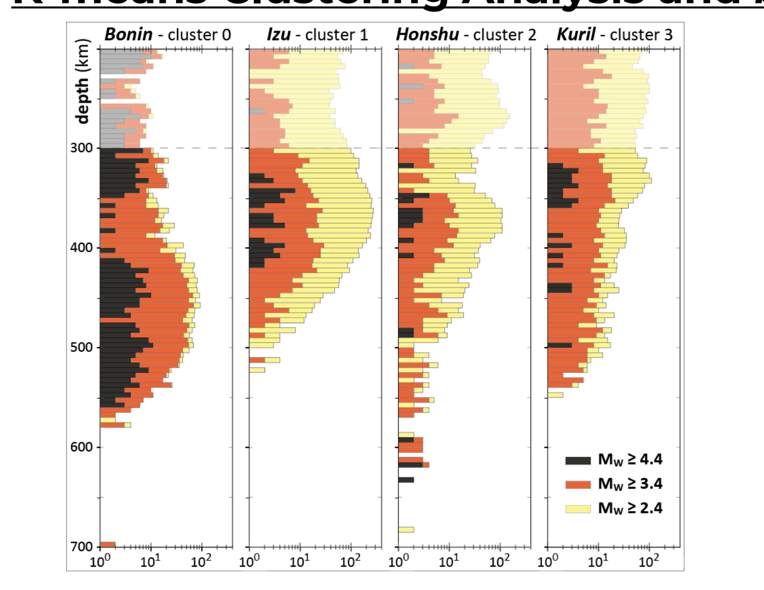

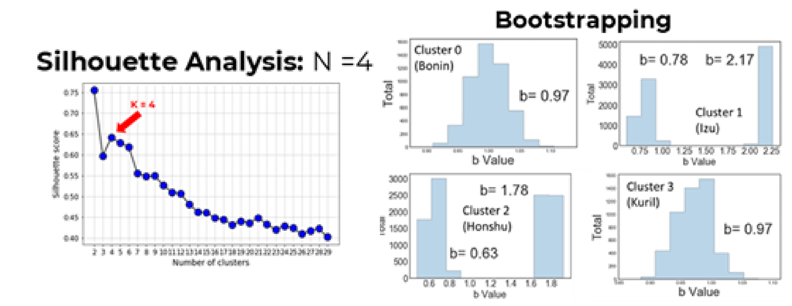

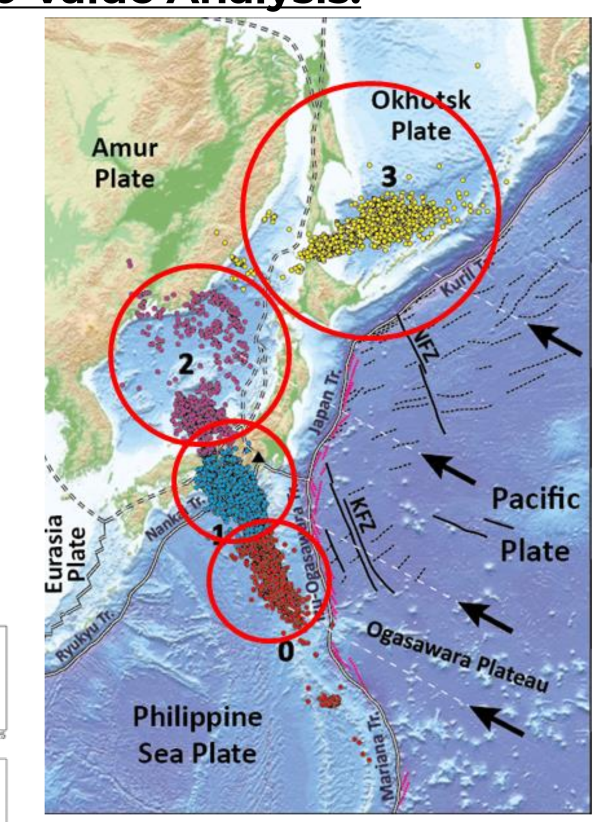

Mao et al. (in revision)

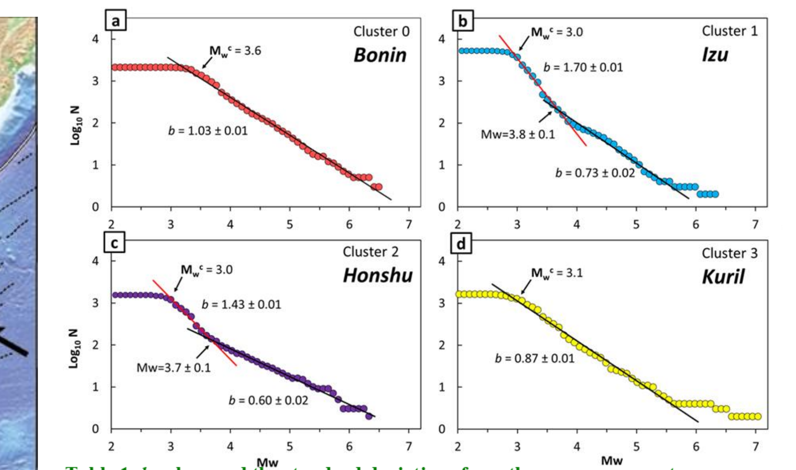

Table 1. *b* values and the standard deviations from three measurements

Region	b_0	σ_{b_0}	b_1	σ_{b_1}	b_2	σ_{b_2}
Kuril	0.97	0.01	0.87	0.01	0.92	0.01
Honshu*	1.72	0.02	1.43	0.01	1.57	0.01
Honshu**	0.65	0.02	0.60	0.02	0.62	0.02
Izu*	2.11	0.01	1.70	0.01	1.89	0.01
Izu**	0.80	0.03	0.73	0.02	0.77	0.02
Bonin	1.09	0.01	1.03	0.01	1.03	0.01

* Mw < 3.8
** Mw > 3.8
The b_0, b_1 and b_2 values are described in section 2.2.
The σ_{b_i} are the standard deviations for each distribution.

Spectral and GMM Clustering Analysis:

Table 2. *b* values and their errors from three measurements (Spectral Clustering, N=5)

Region	b_0	σ_{b_0}	b_1	σ_{b_0}	b_2	σ_{b_2}
Kuril	0.97	0.01	0.87	0.01	1.00	0.01
Honshu*	1.70	0.02	1.42	0.01	1.43	0.01
Honshu**	0.66	0.02	0.61	0.02	0.61	0.02
Izu*	2.10	0.01	1.69	0.01	1.71	0.01
Izu**	0.79	0.02	0.72	0.02	0.73	0.02
Bonin	0.93	0.01	0.84	0.01	0.95	0.01

Table 3. *b* values and their errors (Gaussian Mixture Models Clustering, N=4)

Region	b_0	σ_{b_0}	b_1	σ_{b_0}	b_2	σ_{b_2}
Kuril	0.97	0.01	0.87	0.01	0.88	0.01
Honshu*	1.70	0.02	1.42	0.01	1.43	0.02
Honshu**	0.65	0.02	0.61	0.02	0.61	0.02
Izu*	2.17	0.01	1.74	0.01	1.76	0.01
Izu**	0.83	0.03	0.76	0.02	0.76	0.03
Bonin	1.09	0.01	0.97	0.01	0.97	0.01

Comparison of Three Clustering Methods:

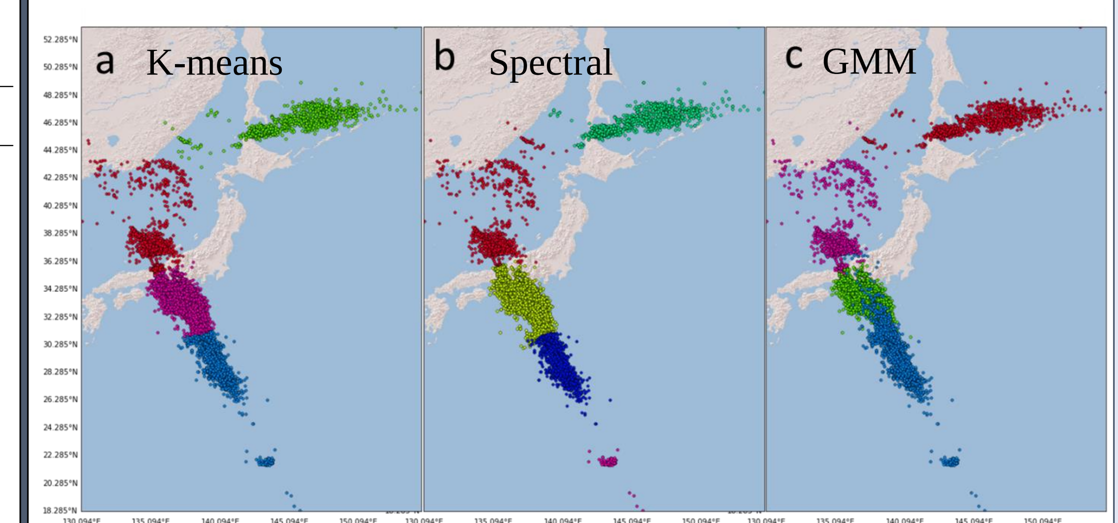

Three clustering methods generated similar clustering maps. The b-value analysis results are also similar. The clustering analysis of the JMA catalog is robust.

b-value analysis with CMT and IRIS catalogs :

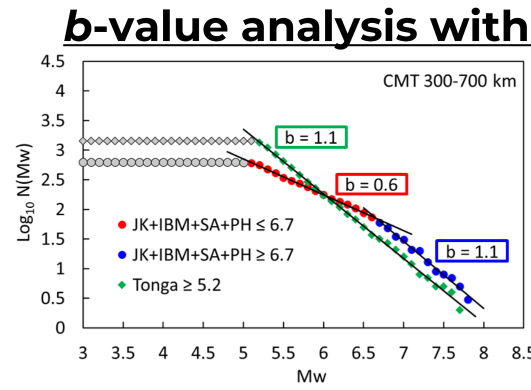

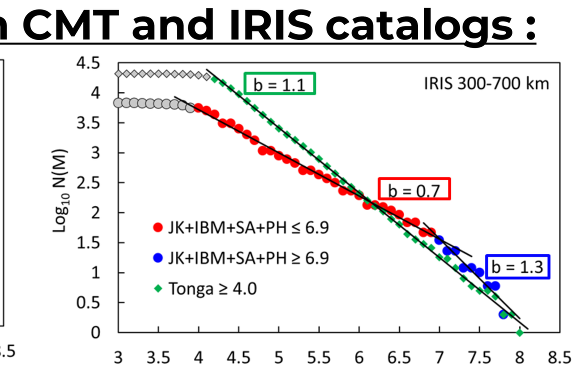

- IRIS and CMT catalogs show similar earthquake distributions
- Warm subduction zones show a change of b-values at Mw~6.8
- Cold Tonga subduction zone has a constant b-value of ~1.1

In JMA catalog, a new kink at Mw 3.8 was observed, in addition to the kink at Mw 6.5 in CMT and IRIS catalogs.

Two *b*-value Kinks indicate two different rupture dimension thresholds.

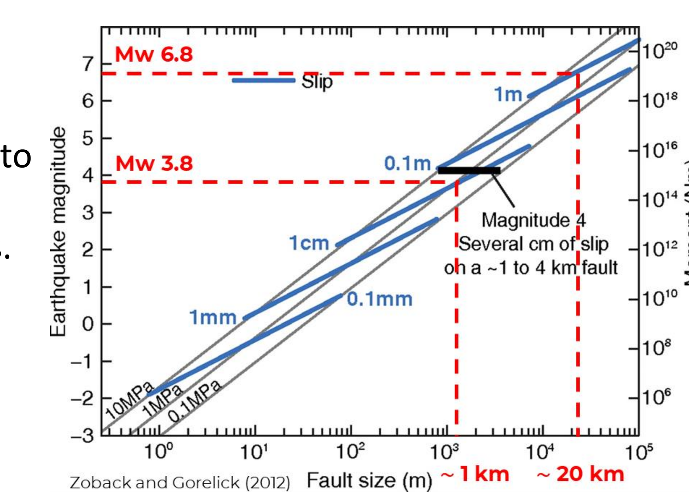

Conclusion:

- Unsupervised machine learning approaches facilitate the unbiased clustering of deep-focus earthquakes from the JMA catalog.
- The *b*-value kink at Mw~3.8 provides strong evidence for phase transformational faulting triggering deep-focus earthquakes in an unstable rim of the metastable olivine wedge with a width of ~1 km.
- In the highly reactive halo, water acts as a catalyst for transformational faulting, resulting in higher *b*-values in the Honshu and Izu slabs for Mw < 3.8.
- We speculate that the *b*-value kink at Mw~3.8 can be observed in other subduction zones with similar tectonic environments and earthquake catalogs.